Flow-induced coalescence: arbitrarily mobile interface model and choice of its parameters

Ivan Fortelný[1), *)], Josef Jůza[1)]

DOI: dx.doi.org/10.14314/polimery.2015.628

Abstract: Coalescence consists of four steps: approach of droplets pair, drainage of the matrix between the droplets, matrix breakup at critical interdroplet distance, and shape relaxation of a new droplet. This communications is based on research of the second coalescence step in systems, where the driving force is a gradient of flow velocities of matrix, while the droplet approach is slowed down by drainage of the matrix film between droplets. We have recently extended the Jeelani and Hartland equation, combining it with the fully mobile interface model, to a model describing the flow-induced coalescence in the whole viscosity range. We have used the arbitrarily mobile interface model (AMI) name to refer to it. The new AMI method is semi empirical and its dimensionless parameters can be determined more precisely by broader comparison with experiment.

Keywords: flow-induced coalescence, polymer blends, interface mobility, arbitrarily mobile interface.

Koalescencja w przepływie: model interfazy o dowolnej ruchliwości i dobór jego parametrów

Streszczenie: Proces koalescencji składa się z czterech etapów: zbliżanie się do siebie pary kropli, rozpływanie się osnowy pomiędzy kroplami, pękanie osnowy przy krytycznej odległości pomiędzy kroplami oraz łączenie kropli i tworzenie nowej jednej kropli. W artykule przedstawiono analizę drugiego etapu koalescencji, gdzie siła napędowa wynika z istnienia gradientu prędkości przepływu osnowy, a zbliżenie się kropel jest spowolnione przez rozpływanie się warstwy osnowy istniejącej pomiędzy kroplami. W ramach przedstawionej pracy rozszerzono równanie Jeelaniego i Hartlanda, łącząc je z modelem w pełni ruchliwej interfazy (FMI); otrzymano model opisujący koalescencję wywołaną przepływem w całym zakresie lepkości, co określono jako model o dowolnej ruchliwości interfazy (*Arbitrarily mobile interface model*, AMI). Analizowano wpływ doboru parametrów *a* i *b* modelu AMI, dla trzech wartości stosunku lepkości kropel do lepkości osnowy w przepływie ścinającym, na prawdopodobieństwo wystąpienia koalescencji (P_c). Nowy model AMI jest półempiryczny, a jego bezwymiarowe parametry *a* i *b* mogą być określone z większą dokładnością dzięki porównaniu z danymi doświadczalnymi. Zapewnia on lepszy opis zjawiska koalescencji w całym zakresie stosunku lepkości kropel do lepkości osnowy niż powszechnie stosowane modele. Może też służyć jako dodatkowa korekta modelu opisującego koalescencję mniejszych kropli o małej lepkości.

Słowa kluczowe: koalescencja w przepływie, mieszaniny polimerowe, ruchliwość interfazy, interfaza o dowolnej ruchliwości.

Coalescence is one of mechanisms of increasing average size of droplets dispersed in a viscoelastic matrix. It consists in droplets collisions followed by their fusion. The course of coalescence can be split into four steps [1]: 1) approach of the droplets, 2) drainage of the matrix film trapped between the approaching droplets, 3) breakup of the matrix film between the droplets after their approaching to the critical distance, h_c, 4) relaxation of the shape of a droplet formed by the coalescence to the spherical one. The coalescence has various driving forces; that of flow-induced coalescence is a difference in matrix flow velocity in places where respective droplets are located.

This communication is based on research of the second coalescence step using a „ballistic" approximation [2], *i.e.*, interdroplet interactions are neglected until the droplets approach to a very short distance. Subsequently, coalescence is controlled by the competition between velocity of the droplet approach slowed down by drainage of the matrix film trapped between them and speed of rotation around their common center of inertia [3—6]. Effect of drainage can be quantified by the probability P_c that the droplets collision (their touching if all their interactions are neglected) is followed by their fusion (colli-

[1)] Institute of Macromolecular Chemistry of Academy of Sciences of the Czech Republic, Heyrovského nám. 2, CZ 162 06 Praha 6, Czech Republic.

[*)] Author for correspondence; e-mail: fortelny@imc.cas.cz

sion efficiency [4]). P_c is expressed as the ratio of the flux, J_c, of droplets pairs into the contact surface (affected by matrix drainage and droplets rotation) to the flux J_0, of particles that do not interact until collision (in other words, that they would collide in absence of matrix resistance, attraction forces *etc*.)

$$P_c = J_c/J_0 \tag{1}$$

where: J_c can be expressed as [4]

$$J_c = -n^2 \int_{A_c} \mathbf{u} \cdot \mathrm{N} \mathrm{d}S \tag{2}$$

where: n — the droplet number in the unit volume, N — outward unit normal to the spherical contact surface, A_c — upstream interception area, **u** — velocity, dS — the surface element. To evaluate J_c, one has to find the range of initial positions that a droplet pair has to occupy to coalesce; this is determined by calculation of their trajectory: the droplet pair coalesces if droplets approach to the critical distance h_c or closer, where the matrix film breaks up and both droplets can merge.

An exhausting description of the coalescence process is too difficult. Therefore, published models use approximations. Basic models describe droplets as small spheres and study their trajectories. However, droplets can flatten when they approach to a closer distance, which markedly changes resistance of the matrix drained by the droplets. This droplet flattening was described long ago, and Elmendorp and Van der Vegt [3] published their way to combine these equations with those for spherical droplets. Matrix drainage between highly flattened droplets is described using approximate models of the matrix drainage between parallel plates for different ratios of viscosities of the dispersed phase and matrix: fully mobile (FMI; for the droplets with much lower viscosity than the matrix), partially mobile (PMI; for the droplets and matrix of similar viscosity), or immobile (IMI; for hard spheres in a viscous matrix) interface models [1, 7]; however, these models do not converge one to another with changing viscosity ratio. Jeelani and Hartland derived [8] an equation for matrix drainage to describe systems with finite viscosity ratios of both phases; the equation converges to the equation for the IMI model at high droplet viscosity ratios.

We have proposed a model describing matrix drainage in the full range of viscosity ratios [9]. The model is based on the Jeelani and Hartland model and is described below (Model details / Arbitrarily mobile interface model).

MODEL ASSUMPTIONS

System geometry — shear and extensional flow

Due to difficulty of modelling and experimental determination of the coalescence in complex flow fields, theoretical and experimental studies of the flow induced coalescence deal often, including our work, with simple linear flows: shear and extensional [10].

Extensional flow

Measurements of molten polymer materials in extensional flow are important for practice. Principles of the measurement and constructions of rheometers are described in ref. [10]. In Cartesian coordinates, velocity, **u**, of steady uniaxial extension can be expressed as $\mathbf{u} = \dot{\varepsilon}(-x, -y, 2z)$, where rate of extension, $\dot{\varepsilon}$, is constant. The droplets position is described in terms of radius of droplets in a undeformed state, R, distance between droplets surfaces, h, and angle between flow direction and the line connecting the droplet centres, θ. Our studies are based on the previous paper [11].

Droplets fuse for initial angles ranging between the right angle and an acute limit angle $\theta_0^{(m)}$. The following equation is valid for P_c:

$$P_c = \frac{3\sqrt{3}}{4} \sin\theta_0^{(m)} \sin\left(2\theta_0^{(m)}\right) \tag{3}$$

The coalescence driving force is expressed by the following formula [11]:

$$F = K\pi\eta_m \dot{\varepsilon} R^2 (1 - 3\cos^2\theta) \tag{4}$$

where: η_m — matrix viscosity, K — a function of viscosity ratio $p = \eta_d/\eta_m$:

$$K = K_\infty \frac{2 + 3p}{3(1 + p)} \tag{5}$$

where: K_∞ — the value of K for $p \to \infty$, very weakly dependent on interdroplet distance. $K_\infty = 12$ for force on rigid spheres in unperturbed flow and $K_\infty = 12.24$ for force on doublet of touching spheres [12, 13] used in our numerical calculations.

Shear flow

The shear flow in rotational and capillary rheometers is most frequently used for determination of flow properties of molten polymer materials. In Cartesian coordinates, the shear flow can be described as flow with velocity in x direction having gradient in y direction, z is neutral axis. It is assumed in this coalescence model that the velocity gradient, *i.e*., shear rate is constant. In our papers [9, 13], droplets movement and mutual position were described using shear rate, $\dot{\gamma}$, radius R, surfaces distance h, polar angle, θ, and azimuth ϕ (see Fig. 1 in ref. [13]). In this case, P_c is calculated as:

$$\begin{aligned} P_c &= 3 \int_0^{\pi/2} \int_0^{\phi_M(\theta_0)} \frac{\sin 2\phi_0}{2} \sin^3\theta_0 \, \mathrm{d}\phi_0 \, \mathrm{d}\theta_0 = \\ &= 3 \int_0^{\pi/2} \frac{1 - \cos\left[2\phi_M(\theta_0)\right]}{4} \sin^3\theta_0 \, \mathrm{d}\theta_0 \end{aligned} \tag{6}$$

where: ϕ_0, θ_0 — azimuth and polar angle at the beginning of coalescence, $\phi_M(\theta_0)$ — maximum azimuth angle for a certain initial polar angle θ_0 at which the droplets fuse, it has to be calculated numerically for each θ_0 in most models.

The coalescence driving force is expressed by the following formula [13]:

$$F = \frac{K}{2}\pi\eta_m\dot{\gamma}R^2\sin^2\theta\sin(2\phi) \tag{7}$$

Movement description

Rotation

The droplets rotation around centre of inertia was described by Wang *et al*. [4] for extensional flow as:

$$\frac{\mathrm{d}\theta}{\mathrm{d}t} = -3(1-\beta)\dot{\varepsilon}\sin\theta\cos\theta = -\dot{\varepsilon}D_e(\theta) \tag{8}$$

and for shear flow as:

$$\frac{\mathrm{d}\phi}{\mathrm{d}t} = \dot{\gamma}\left[\sin^2(\phi) + \frac{\beta}{2}\cos(2\phi)\right] = \dot{\gamma}D(\phi) \tag{9}$$

$$\frac{\mathrm{d}\theta}{\mathrm{d}t} = -\dot{\gamma}\frac{(1-\beta)}{4}\sin(2\theta)\sin(2\phi) \tag{10}$$

The current polar angle can be expressed using droplet's initial position and the azimuth. Division of equation (10) by equation (9) and following integration leads to:

$$\theta = \mathrm{arctg}\left(\mathrm{tg}\theta_0\left[\frac{(1-\beta)\sin^2\phi_0 + \beta/2}{(1-\beta)\sin^2\phi + \beta/2}\right]^{\frac{1}{2}}\right) \tag{11}$$

where: β — a function of the ratio of the distance between droplets centers and droplet radius, as well as of viscosity ratio p and of droplet size ratio. However, we have used for simplicity constant $\beta = 0.075$ (average value following from ref. [4]) in our numerical calculations, because P_c is insensitive to value of β for parameters considered in our calculations [13].

Spherical droplets approaching

We [13] suggested an approximation to involve viscoelastic properties of matrix, consisting in using $F + \tau_m\,\mathrm{d}F/\mathrm{d}t$ instead of simple F for drag force of particles. Zhang and Davis [14] expressed approaching of close spherical droplets; their formula after adding the viscoelastic component becomes:

$$-\left(\frac{\mathrm{d}h}{\mathrm{d}t}\right)_{\mathrm{Sp}} = \frac{2h\left(F + \tau_m\frac{\mathrm{d}F}{\mathrm{d}t}\right)}{3\pi\eta_m R^2 g(m)} \tag{12}$$

where: h — interdroplet distance and $g(m)$ is given by:

$$g(m) = \frac{1 + 0.402m}{1 + 1.711m + 0.461m^2} \tag{13}$$

with m defined as:

$$m = \frac{\eta_m}{\eta_d}\left(\frac{R}{2h}\right)^{\frac{1}{2}} \tag{14}$$

where: η_m, η_d — viscosities of the matrix and droplets, respectively.

Flattened droplets approaching

In earlier text, several models [1, 6—8] describing drainage of matrix between highly flattened droplets have been mentioned.

The fully mobile interface (FMI) model for droplets of low viscosity treats velocity of the flowing matrix between droplets as uniform across the section. Approaching is described as [1, 7]:

$$-\left(\frac{\mathrm{d}h}{\mathrm{d}t}\right)_{\mathrm{FMI}} = \frac{2\sigma h}{3\eta_m R} \tag{15}$$

where: σ — interfacial tension.

The immobile interface (IMI) model for viscous droplets supposes zero flow velocity in contact with droplet surface and maximum velocity in the middle of interdroplet distance [1, 7].

$$-\left(\frac{\mathrm{d}h}{\mathrm{d}t}\right)_{\mathrm{IMI}} = \frac{8\pi\sigma^2h^3}{3\eta_m R^2\left(F + \tau_m\frac{\mathrm{d}F}{\mathrm{d}t}\right)} \tag{16}$$

The partially mobile interface (PMI) model accounts for constant flow velocity in the whole space between both surfaces, but also for some flow inside droplets. The following equation for systems with similar viscosities of both phases is valid for the droplet approach [1, 7]:

$$-\left(\frac{\mathrm{d}h}{\mathrm{d}t}\right)_{\mathrm{PMI}} = \frac{4(2\pi)^{1/2}\sigma^{3/2}h^2}{\eta_d R^{3/2}\left(F + \tau_m\frac{\mathrm{d}F}{\mathrm{d}t}\right)^{1/2}} \tag{17}$$

The Jeelani-Hartland (JH) [6, 8] model uses similar formula as IMI, but contains a coefficient regarding both droplets and matrix viscosity. For matrix viscosity negligible in comparison with droplet viscosity, the formula becomes identical with IMI.

$$-\left(\frac{\mathrm{d}h}{\mathrm{d}t}\right)_{\mathrm{JH}} = \frac{8\pi\sigma^2h^3}{3\eta_m R^2\left(F + \tau_m\frac{\mathrm{d}F}{\mathrm{d}t}\right)}\left(1 + 3C\frac{\eta_m}{\eta_d}\right) \tag{18}$$

where: C — dimensionless circulation length of the order of 1 [8]. It is constant in the Jeelani-Hartland model, and its replacement by a suitable function is an idea of our AMI model described later.

MODEL DETAILS

Movement descriptions

Since the right members in the equations (8) and (9) do not change their signs between zero angle and right angle, the droplet approach can be simplified to trajectory description as a dependence of interdroplet distance on angle (azimuth for shear rate). If the driving-force term for the shear flow is rewritten as:

$$F + \tau_m\frac{\mathrm{d}F}{\mathrm{d}t} = K\pi\eta_m\dot{\gamma}R^2\left[Q(\theta,\phi) + \tau_m\dot{\gamma}S(\theta,\phi)\right] \tag{19}$$

and for the extensional flow analogically:

$$F + \tau_m\frac{\mathrm{d}F}{\mathrm{d}t} = K\pi\eta_m\dot{\varepsilon}R^2\left[Q_e(\theta) + \tau_m\dot{\gamma}S_e(\theta)\right] \tag{20}$$

and $D(\phi)$ from equation (8) or (9) is used, the following equations in the universal shape for both the extensional (quantities with e subscript) and shear flow are obtained:

$$-\left(\frac{\mathrm{d}h}{\mathrm{d}t}\right)_{\mathrm{Sp}} = G_{\mathrm{Sp}}\frac{h}{g(m)}\frac{Q(\theta,\phi) + \tau_m\dot{\gamma}S(\theta,\phi)}{D(\phi)} \tag{21}$$

for spherical droplets,

$$-\left(\frac{\mathrm{d}h}{\mathrm{d}t}\right)_{\mathrm{FMI}} = G_{\mathrm{FMI}}\frac{h}{D(\phi)} \tag{22}$$

for the fully mobile interface,

$$-\left(\frac{\mathrm{d}h}{\mathrm{d}t}\right)_{\mathrm{IMI/JH}} = G_{\mathrm{IMI/JH}}\frac{h^3}{D(\phi)[Q(\theta,\phi)+\tau_m\dot{\gamma}S(\theta,\phi)]} \tag{23}$$

for the immobile interface or Jeelani and Hartland model, and

$$-\left(\frac{\mathrm{d}h}{\mathrm{d}t}\right)_{\mathrm{PMI}} = G_{\mathrm{PMI}}\frac{h^2}{D(\phi)[Q(\theta,\phi)+\tau_m\dot{\gamma}S(\theta,\phi)]^{1/2}} \tag{24}$$

for the partially mobile interface, where:

$$G_{\mathrm{Sp}} = \frac{2}{3}K \tag{25}$$

$$G_{\mathrm{FMI}} = \frac{2\sigma}{3\eta_m R\dot{\gamma}} \tag{26}$$

$$G_{\mathrm{IMI}} = \frac{8\sigma^2}{3K(\eta_m\dot{\gamma}R^2)^2} \tag{27}$$

$$G_{\mathrm{JH}} = \frac{8\sigma^2}{3K(\eta_m\dot{\gamma}R^2)^2}\left(1+3C\frac{\eta_m}{\eta_d}\right) \tag{28}$$

$$G_{\mathrm{PMI}} = \frac{4\sqrt{2}\sigma^{3/2}}{K^{1/2}\eta_d\eta_m^{1/2}\dot{\gamma}^{3/2}R^{5/2}} \tag{29}$$

$$Q(\theta,\phi) = \frac{1}{2}\sin^2\theta\sin 2\phi \tag{30}$$

$$S(\theta,\phi) = \frac{1-\beta}{8}(\sin 2\theta\sin 2\phi)^2 + D(\phi)\sin^2\theta\cos 2\phi \tag{31}$$

$$Q_e(\theta) = 1-3(\cos\theta)^2 \tag{32}$$

$$S_e(\theta) = -\frac{9}{2}(1-\beta)[\sin(2\theta)]^2 \tag{33}$$

These equations are used to calculate the droplet trajectory as mentioned in introduction to find out whether they reach the distance h_c or shorter, which means their fusion.

Combining flat and spherical droplets equations

When the driving force is low, the droplets keep practically spherical shape. Conditions for validity of equations (22)—(24) are not met and equations (23) and (24) diverge. Therefore, combination of equation (21) for spherical particles is to be used together with equations (22)—(24). Elmendorp *et al.* [3] used an additive inversion equation:

$$\left(\frac{\mathrm{d}h}{\mathrm{d}\phi}\right)^{-1} = \left(\frac{\mathrm{d}h}{\mathrm{d}\phi}\right)_{\mathrm{Sp}}^{-1} + \left(\frac{\mathrm{d}h}{\mathrm{d}\phi}\right)_{\mathrm{F}}^{-1} \tag{34}$$

This equation leads to overestimation of the resistance against matrix drainage when both its components are equal. We therefore decided to evaluate derivatives in each point of the curve and to use that of lower value:

$$\left(\frac{\mathrm{d}h}{\mathrm{d}\phi}\right) = \min\left\{-\left(\frac{\mathrm{d}h}{\mathrm{d}\phi}\right)_{\mathrm{Sp}};-\left(\frac{\mathrm{d}h}{\mathrm{d}\phi}\right)_{\mathrm{F}}\right\} \tag{35}$$

More detail discussion of this choice of the calculation method can be found in [13].

However, this modification caused a necessity of using numerical solution instead of the analytical one. This way of formulae combination has been used in all our recent works including this one, it will be referred to as formulae switching thereafter. During our current research, it has been specified that, in case of negative driving force, the formula for spherical particles is to be used in this point.

Arbitrarily mobile interface model

Each of the basic models (IMI, FMI, PMI) covers its range of ratios of droplets and matrix viscosities, and do not pass one to another with viscosity change. Moreover, range of their applicability has not been established so far. The Jeelani and Hartland model converges to the IMI model with increasing droplets viscosity.

In our recent work [9], we have introduced a new model to cover the whole viscosity ratio range. We have used the arbitrarily mobile interface model (AMI) name to refer to it. It is based on the Jeelani and Hartland model (23), where instead of constant *C* parameter in equation (28), such function of viscosity ratio is to be chosen that the equation converges to the IMI model for high droplets viscosity and to the FMI model (22) for low droplets viscosity in comparison with the matrix viscosity:

$$C = a\left\{1-\exp\left[-\frac{p}{3a}\left(\frac{RF_c}{4\pi h^2\sigma}-1+bp\right)\right]\right\} \tag{36}$$

The model uses two adjustable dimensionless parameters. The *a* parameter shifts the resulting model between the FMI and IMI models. The primary purpose of the *b* parameter was to prevent dividing by zero or rooting negative numbers, which happened for the originally developed formula without this parameter.

The *a* parameter has appeared to be suitable to fit calculated results to experimental data or results obtained by other procedures. Naturally, the basis is that the FMI and IMI models comply with experimental data in both limit cases. It appears as a possible drawback that *a* affects the same system differently for different droplet sizes or shear rates; with intermediate *a*, the results incline to the FMI model for smaller, while to the IMI model for larger droplets. The *b* parameter exhibits an observable influence on results only for droplets less viscous than the matrix.

This communication presents a detailed study of the effect of the *a* and *b* parameters on P_c and discussion of the methods of numerical calculation for the extensional flow.

Boundary conditions for direct calculation in extensional flow

As mentioned in earlier text, the collision efficiency is expressed by equations (3) and (6) with the limit initial angles from that a droplet pair coalesces.

In the original extensional-flow model [11], the limit angle $\theta_0^{(m)}$ was calculated by backward integration from final position θ* (an angle of closest approach), with boundary condition of critical inter-surface distance h_c (see end of introduction) at this angle, in direction of increasing angles to initial inter-surface distance h_0. In the Newtonian model without attractive forces, the closest approach angle is θ* = arccos (1/√3) = arctg (2). The critical distance can be expressed [1] as:

$$h_c = \left(\frac{AR}{8\pi\sigma}\right)^{\frac{1}{3}} \tag{37}$$

where: A — the Hamaker constant.

A universal way to find limit initial angles is based on integration of the drop trajectory from possible initial positions. For the shear flow, one has to find out whether droplets coalesce for a given polar angle θ from the right-angle initial azimuth [usually, they do not, otherwise $\phi_M = \pi/2$ in equation (6)], and from zero azimuth. If they do not coalesce from zero initial azimuth, then $\phi_M = 0$; else the limit azimuth is obtained by methods like the bisection method. Similarly for the extensional flow, if droplets do not coalesce even at right initial angle, then $\theta_0^{(m)} = \pi/2$ in equation (3). Droplets cannot coalesce from initial angles below θ*, since they always move away from each other. Therefore, $\theta_0^{(m)}$ can be found using *e.g.* the bisection method between zero (or θ*) and right angle.

The backward integration is much more elegant and involves less computation, however, its usage for the shear flow to find the limit azimuth ϕ_M for given polar angle is complicated by changes of polar angle during the process.

When using more complicated formulae (*e.g.* viscoelastic matrix, attractive forces), the interdroplet distance may not reach just one minimum necessary for estimation of collision efficiency using backward integration. The forward integration from possible initial positions with bisection methods as mentioned in previous paragraph is to be used. However, θ* determination for more models can be useful to enable using shorter backward integration also for more complicated models of extensional-flow induced coalescence.

The principle of formulae switching according to lower d*h*/d*t* determines equation (21) for spherical particle as effective in this point. This means that the condition

$$Q_e(\theta^*) + \tau_m \dot{\varepsilon} S_e(\theta^*) = 0 \tag{38}$$

applies. If we substitute $Y = \mathrm{tg}^2(\theta^*)$ and if we group physical constants into parameter

$$\Omega = 9\tau_m \dot{\varepsilon}(1-\beta) \tag{39}$$

we have

$$1 - \frac{3}{(1+Y)} - \frac{2\Omega Y}{(1+Y)^2} = 0 \tag{40}$$

which can be transformed to

$$Y^2 - (2\Omega + 1)Y - 2 = 0 \tag{41}$$

the positive solution is

$$Y = \Omega + \frac{1}{2} + \sqrt{\Omega^2 + \Omega + \frac{9}{4}} \tag{42}$$

The van der Waals attractive forces are approximately [15]

$$F_W \cong \frac{AR}{12h^2} \tag{43}$$

Taking them into account, equation (38) extends to:

$$Q_e(\theta) + \frac{A}{12K\pi\eta_m \dot{\varepsilon} R h^2} + \tau_m \dot{\varepsilon} S_e(\theta) = 0 \tag{44}$$

Substituting

$$\left(1 + \frac{A}{12K\pi\eta_m \dot{\varepsilon} R h^2}\right) = \alpha \tag{45}$$

leads analogically to

$$Y^2 - \frac{(2\Omega + 3 - 2\alpha)}{\alpha} Y - \frac{3}{\alpha} + 1 = 0 \tag{46}$$

with solutions.

$$Y = \frac{\Omega}{\alpha} + \frac{3}{2\alpha} - 1 \pm \sqrt{\frac{\Omega^2}{\alpha^2} + \frac{\Omega}{\alpha}\left(\frac{3}{\alpha} - 2\right) + \frac{9}{4\alpha^2}} \tag{47}$$

$$\theta^* = \mathrm{arctg}\sqrt{\frac{9\tau_m \dot{\varepsilon}(1-\beta)}{\alpha} + \frac{3}{2\alpha} - 1 + \sqrt{\frac{[9\tau_m \dot{\varepsilon}(1-\beta)]^2}{\alpha^2} + \frac{9\tau_m \dot{\varepsilon}(1-\beta)}{\alpha}\left(\frac{3}{\alpha} - 2\right) + \frac{9}{4\alpha^2}}} \tag{48}$$

The direct backward integration can be used if equation (47) has just one positive solution. If attractive forces are so strong that they prevail over matrix resistance in critical distance, the closest approach cannot take place in h_c. In such a case, there exists the shortest distance where droplets can stop approaching, see equation (37).

RESULTS AND DISCUSSION

AMI model characteristics

The most suitable values of the *a* and *b* parameters can be sought through comparison with the IMI, FMI, PMI models and Jeelani and Hartland formula with *C*=1. Comparison of the dependence of P_c on drop size *R* is made for matrix viscosity η_m = 1 kPa · s, droplets viscosities η_d changing from 0.1 kPa · s to 10 kPa · s, interfacial tension 1 mN/m, shear rate 0.1 s^{-1}, K_∞ = 12.24, initial distance $h_0 = 10\,R$, and critical distance h_c determined by formula using Hamaker constant A = 5·10^{-17} J. Figures 1 and 2 show the situation for the shear flow.

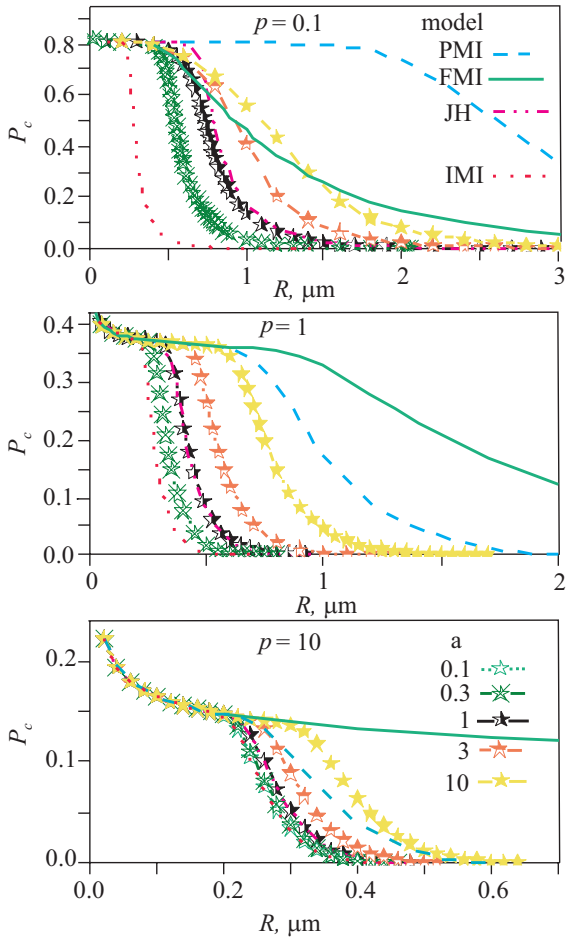

Fig. 1. Influence of *a* parameter change on calculated collision efficiency, compared with other models, for ratios η_d/η_m from 0.1 to 10 and *b* = 1; other parameters given in text

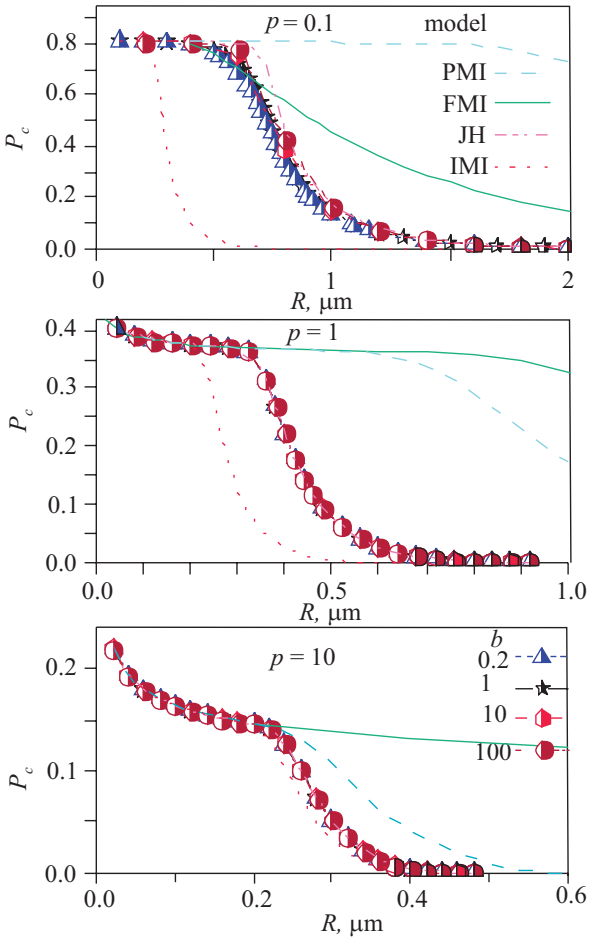

Fig. 2. Influence of *b* parameter change on calculated collision efficiency, compared with other models, for ratios η_d/η_m from 0.1 to 10, *a* = 1, other parameters given in text

Figure 1 shows what happens with changing the *a* parameter. For lower droplet viscosity, where FMI is a proper model, any change in *a* has negligible influence for smaller droplets having higher collision efficiency; a decrease in *a* lowers collision efficiency making its dependence on droplet size sharper. For higher droplet viscosity, where the system becomes more similar to that described by the IMI model, increasing *a* shifts the dependence of probability on droplet size to larger sizes, keeping essentially the dependence shape. The dependence for equal viscosities (the PMI and Jeelani and Hartland models are proper ones) shows that decreasing *a* shifts the dependence closer to that according to the Jeelani and Hartland model and, therefore, to the IMI model, while increasing *a* makes the dependence more similar to the FMI model. The *a* parameter can thus serve to balance the AMI model between FMI and IMI adjusting to experimental data, if available. However, we can also see that this balancing is not uniform: with intermediate *a*, the dependence may be closer to that according to the FMI model for smaller sizes with higher P_c, but still follows the JH and IMI models for larger *R* with smaller P_c. For the smallest P_c, where it decreases with growing droplet size very slowly in the FMI model, our AMI model differs from FMI most significantly. Some combinations of too low *a* and *b* parameters lead to a negative value of $(RF_c/4\pi h^2\sigma) - 1 + bp$, therefore to negative *C* value, and to the failure of the model. The *b* parameter has been designed just to avoid this failure.

Figure 2 demonstrates the influence of the *b* parameter on the obtained results. The plot for higher droplet viscosity ($p = 10$) exhibits only negligible, if any, dependence of collision efficiency on the used *b* parameter. Somewhat different is the situation for low droplet viscosities, when a low *b* parameter provides lower P_c, making its dependence on *R* similar to that of the FMI model, while high *b* values increase obtained P_c with its dependence on *R* similar to the IMI model. For comparable viscosities of droplets and the matrix, influence of *b* changes are hardly observable; let us note that even the above mentioned changes for low droplets viscosities are due to changes in *b* by several orders of magnitude. While the change in *a* affects the dependence in the range of low P_c and larger *R*, the change in *b* modifies results in the opposite part of the curve for smaller droplets having higher P_c.

In our recent paper [9], we have compared results obtained using the models described above with the results of Rother and Davis [16] who used a trajectory analysis

method with droplet flattening as a perturbation. We have found $a = 8$ and $b = 1$ to provide results in much better agreement with Rother than other models.

Extensional flow by direct backward trajectory integration

As mentioned in earlier text, the direct backward integration is a much more straightforward and quick method to obtain collision efficiency than a robust but slower universal method. It provides results differing by 0.002 at most from those obtained by integration in the direction of motions combined with the bisection method. An exception is when equation (47) has no solution, but also if some of rooted expressions in equation (48) are close to zero.

The direct integration can be used if dependence of droplets distance on angle has just one minimum. This is connected with existence of just one point where $F+\tau_m \, dF/dt$ is zero and grows with the angle. Figure 3 shows that the dependence of expression in equation (38) or (44) on angle in Newtonian system (N curve) is monotonous from -2 to 1; therefore it is sure that there is just one value of θ*.

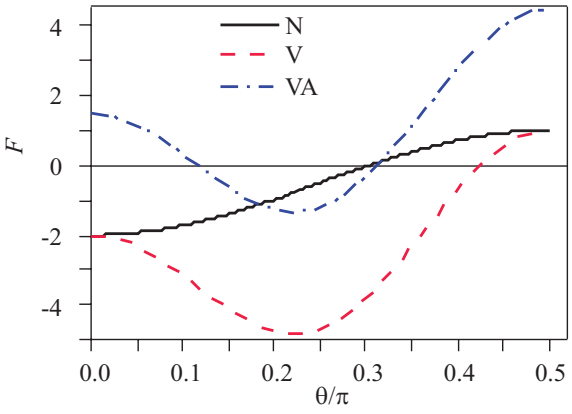

Fig. 3. Force on angle dependence for extensional flow, β = 0.075, $\dot{\varepsilon}$ = 0.1 s^{-1}; N: Newtonian model (τ_m = 0 s, A = 0 J), V: viscoelastic model, τ_m = 10 s, A = 0 J, VA: viscoelastic model including attractive forces, τ_m = 10 s, A = 2·10^{-19}J

If we use the viscoelastic model, $S_e(\theta)$ given by equation (33) is zero in both zero and right angle and has one minimum, which means that equation (38) has just one solution. This is shown as the V curve in Fig. 3 representing the dependence of the left member of equation (38) on angle for shear rate 0.1 s^{-1} and relaxation time 10 s. From this point of view, the direct integration can be used.

If we consider too strong attractive forces, it is intuitively clear that droplets in any initial position coalesce since attractive forces overpower repulsive ones. The VA curve in Fig. 3 shows the left member of equation (44) for shear rate 0.1 s^{-1}, relaxation time 10 s and Hamaker constant 2·10^{-19} J. We can see that the driving force is zero for two different angles. Dependence of droplets distance on angle may also be nonuniform and, therefore, the direct integration would be quite dubious.

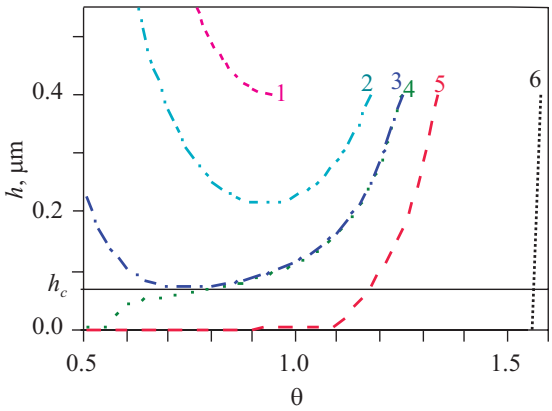

Fig. 4. Trajectory of droplet pair for Newtonian system with strong attractive forces in extensional flow expressed as change of distance *h* with angle θ, AMI model, β = 0.075, *R* = 40 nm, $\dot{\varepsilon}$ = 0.1 s^{-1}, *a* = 8, *b* = 1, A = 5·10^{-18} J, h_0 = 0.4 μm; the direction of movement is to lower θ, initial angle θ_0 increases with curve number from $\theta_0 < \theta^*$ (curve 1) to θ_0 near to π/2 (curve 6)

The droplet trajectory in the Newtonian model without attractive forces looks like curves 1—3 and 6 in Fig. 4. A droplet in the initial position near to the right angle (curve 6) approaches closer than to the critical distance h_c and coalesces. A droplet in the initial position below θ* moves away from the beginning (curve 1). Droplets starting from intermediate positions approach to some minimal distance and then they move apart (curves 2 and 3); they coalesce if only this minimum distance is equal or less than the critical distance. The backward integration method supposes that this minimum will be just at the critical distance if the droplet's initial position is at the limit angle. However, the attraction forces cause the trajectory like in curves 4 and 5. It could be possible to solve the condition that both the first and second derivatives of distance according to angle are zero; however, the latter should be solved numerically with big uncertainty in the angle. Therefore, the practical applicability of the backward integration depends on existence of real solution of equation (48).

It also appeared that the angle need not change uniformly with time for long relaxation times or strong attractive forces. Therefore, whole simplification to the dependence of distance on angle is improper for too strong attractive or elastic forces. The simultaneous integration of all space coordinates according time should be used in such cases.

A consequence of including attractive forces is that there are some initial positions, from which the droplets

coalesce, although they do not coalesce in absence of interactions. This means that determined collision efficiency P_c can exceed 1. In this light, the collision efficiency — term used by Rother and Davis [16] or Wang *et al*. [4] — seems to be more suitable.

CONCLUSIONS

The new AMI model of coalescence provides a better description of the coalescence for the whole range of viscosity ratios than commonly used models. The model has two parameters, the *a* parameter is suitable to basic fitting of the model to known experimental data, while the *b* parameter introduced primarily in order to avoid rooting of negative numbers can be used for additional adjustment for smaller droplets in the domain of low droplet viscosities.

Application of the models taking into account more system parameters limits the usability of direct methods to calculate limit initial angle and therefore collision efficiency. However, if the equation for the closest droplets approach at the distance equal to the critical one has real solution, the direct method can be used.

ACKNOWLEDGMENT

The authors are grateful for the financial support of the Grant Agency of the Czech Republic (grant no. P106/11/1069).

REFERENCES

[1] Chesters A.K.: *Chemical Engineering Research and Design: Transactions of the Institution of Chemical Engineers* **1991**, *69*, 259.

[2] Milner S.T., Xi H.: *Journal of Rheology* **1996**, *40*, 663. http://dx.doi.org/10.1122/1.550731

[3] Elmendorp J.J., Van der Vegt A.K.: *Polymer Engineering and Science* **1986**, *26*, 1332. http://dx.doi.org/10.1002/pen.760261908

[4] Wang H., Zinchenko A.Z., Davis R.H.: *Journal of Fluid Mechanics* **1994**, *265*, 161. http://dx.doi.org/10.1017/S0022112094000790

[5] Janssen J.M.H., Meijer H.E.H.: *Polymer Engineering and Science* **1995**, *35*, 1766. http://dx.doi.org/10.1002/pen.760352206

[6] Fortelný I. in: "Micro- and Nanostructured Multiphase Polymer Blends Systems" (Eds. Harrats C., Thomas S., Groeninckx G.), Taylor and Francis, Boca Raton 2006, p. 43. http://dx.doi.org/10.1201/9781420026542.ch2

[7] Janssen J.M.H.: "Dynamics of liquid–liquid mixing", PhD Thesis, Eindhoven University of Technology, The Netherlands, 1993.

[8] Jeelani S.A.K., Hartland S.: *Journal of Colloid Interface Science* **1994**, *164*, 296. http://dx.doi.org/10.1006/jcis.1994.1171

[9] Fortelný I., Jůza J.: *Colloid and Polymer Science* **2013**, *291*, 1863. http://dx.doi.org/10.1007/s00396-013-2917-x

[10] Macosko C. W.: "Rheology: Principles, Measurements and Application", Wiley-VCH, New York 1994.

[11] Fortelný I., Živný A.: *Rheologica Acta* **2003**, *42*, 454. http://dx.doi.org/10.1007/s00397-003-0300-4

[12] Nir A., Acrivos A.: *Journal of Fluid Mechanics* **1973**, *59*, 209. http://dx.doi.org/10.1017/S0022112073001527

[13] Fortelný I., Jůza J.: *Journal of Rheology* **2012**, *56*, 1393. http://dx.doi.org/10.1122/1.4739930

[14] Zhang X., Davis R.H.: *Journal of Fluid Mechanics* **1991**, *230*, 479. http://dx.doi.org/10.1017/S0022112091000861

[15] Fortelný I., Živný A.: *Polymer* **1995**, *36*, 4113. http://dx.doi.org/10.1016/0032-3861(95)90992-B

[16] Rother M.A., Davis R.H.: *Physics of Fluids* **2001**, *13*, 1178. http://dx.doi.org/10.1063/1.1358871

Received 3 X 2014.